

Using Deep Reinforcement Learning to Enhance Channel Sampling Patterns in Integrated Sensing and Communication

Federico Mason, *Member, IEEE*, Jacopo Pegoraro, *Member, IEEE*

Abstract—In Integrated Sensing And Communication (ISAC) systems, estimating the micro-Doppler (mD) spectrogram of a target requires combining channel estimates retrieved from communication with ad-hoc sensing packets, which cope with the sparsity of the communication traffic. Hence, the mD quality depends on the transmission strategy of the sensing packets, which is still a challenging problem with no known solutions. In this letter, we design a deep Reinforcement Learning (RL) framework that fragments such a problem into a sequence of simpler decisions and takes advantage of the mD temporal evolution for maximizing the reconstruction performance. Our method is the first that learns sampling patterns to directly optimize the mD quality, enabling the adaptation of ISAC systems to variable communication traffic. We validate the proposed approach on a dataset of real channel measurements, reaching up to 40% higher mD reconstruction accuracy and several times lower computational complexity than state-of-the-art methods.

Index Terms—Integrated sensing and communication, compressed sensing, micro-Doppler, reinforcement learning

I. INTRODUCTION

In Integrated Sensing And Communication (ISAC), sensing must coexist with primary communication functionalities while introducing minimal overhead and channel occupation. Jointly allocating resources for both communication and sensing tasks requires modifying the communication system [1], which entails high implementation costs on existing wireless network devices. A more affordable approach, termed *communication-centric*, considers communication resources as pre-determined (i.e., non-modifiable), and *reuses* them for sensing purposes, utilizing channel estimates obtained from communication packets [2]. However, communication traffic patterns are typically irregular and sparse in time, due to the channel access and packet transmission protocols. This makes communication signals unsuited for traditional radar sensing applications, which require estimating the channel for extended periods at regular intervals [3].

A widely used example of such applications is the estimation of the micro-Doppler (mD) spectrogram of a target. The latter is a frequency modulation of the received signal due to the movement of different parts of an extended target and enables object recognition and human sensing [4]. To recover the mD from communication packets, Compressed Sensing (CS) techniques are usually employed, exploiting the sparsity of the channel in the Doppler domain [5]. However, when communication traffic is highly irregular, even CS has been shown to provide degraded performance [2]. In such cases, the available channel estimates (or *samples*) obtained

from communication packets can be integrated with *sensing-oriented* transmissions involving only packet headers, as first suggested in [2]. Transmitting sensing packets at suitable times is key to maximizing the mD quality. However, finding optimal sampling times is very challenging due to the complex relation between the sampling pattern and the CS performance.

In radar systems there is full control over the signal transmission times and channel sampling patterns are usually obtained by minimizing the Mutual Coherence (MC) of the CS model matrix [6]. However, MC minimization is a combinatorial problem, and an optimal solution can only be found for specific configurations of the system parameters [7]. Recently, greedy algorithms have been used to find approximate solutions [7] but present high computational complexity that prevents their implementation in real-time. Moreover, none of the state-of-the-art methods works when part of the sampling instants is fixed, a specific issue inherent to ISAC. Hence, two main research challenges arise: (i) MC minimization is computationally complex and does not imply high mD reconstruction quality, (ii) in ISAC, only *part* of the channel sampling instants can be optimized making existing solutions for radars not directly applicable.

In this letter, we tackle the above challenges by exploiting a deep Reinforcement Learning (RL) approach. Specifically, we design a framework where the problem of allocating sensing packets is decomposed into a sequence of decisions made by a RL agent. The agent state includes the planned sampling pattern and the contextual information given by the mD reconstructed in the previous processing window. At each decision step, the agent plans the transmission of new sensing packets and receives a reward that is directly dependent on the quality of the mD reconstruction. This avoids the expensive computation of the MC, significantly reducing the complexity of allocating sensing packets with respect to known methods.

We test the proposed framework on the DISC dataset [8], which contains Channel Impulse Response (CIR) measurements involving human movements. We use the Proximal Policy Optimization (PPO) algorithm to train the agent and compare its performance against two MC minimization algorithms from the recent literature. Experimental results show that our solution obtains significantly better channel sampling patterns than MC-based methods at a fraction of the computational time, demonstrating how data-driven approaches are highly beneficial to optimize ISAC systems.

II. BACKGROUND AND SYSTEM MODEL

In this section, we present the ISAC system where our framework is implemented, and provide background on CS-based mD reconstruction. The system is based on a CIR model adapted from [2], which is compliant with the IEEE 802.11ay ISAC implementation used in the experiments [8].

The authors are with the Department of Information Engineering at the University of Padova, Italy (email: <name>.<surname>@unipd.it). This work was funded by the European Union under the Italian National Recovery and Resilience Plan (NRRP) Mission 4, Component 2, Investment 1.3, CUP C93C22005250001, partnership on “Telecommunications of the Future” (PE00000001 - program “RESTART”).

A. Channel impulse response model

The ISAC system operates with processing windows of W discrete timesteps, indexed by $w \in \mathcal{W} = \{0, \dots, W-1\}$. The timestep duration is denoted by T_c and is assumed short enough that the target Doppler spectrum is constant within a processing window. The CIR $h(\tau, wT_c)$ associated with the window depends on the propagation delay τ and time wT_c , and is expressed as a sum of L Dirac delta components which correspond to the *resolvable* signal propagation paths. Denoting by τ_l the propagation delay of the l -th reflector, and by $\tilde{h}_l[w]$ the l -th CIR component, we have

$$h(\tau, wT_c) = \sum_{l=1}^L \tilde{h}_l[w] \delta(\tau - \tau_l), \quad (1)$$

where we used parentheses (\cdot) and square brackets $[\cdot]$ to denote continuous and discrete-time domains, respectively. Assuming that the multipath parameters are constant within a processing window, we have

$$\tilde{h}_l[w] = \sum_{q=1}^{Q_l} \alpha_{l,q} e^{j2\pi f_{l,q} w T_c}, \quad (2)$$

where $\alpha_{l,q}$ and $f_{l,q}$ are the complex amplitude and Doppler frequency of the q -th scatterer contributing to the l -th resolvable path, respectively. Therefore, each CIR component is expressed as a superposition of Q_l complex exponential terms with frequencies $f_{l,q}$. We observe that the CIR, for a specific delay τ_l , is sparse in the Doppler frequency domain, since $Q_l \ll W$ for typical processing window lengths.

We assume that the ISAC system can detect and track the targets of interest, extracting the corresponding paths from Eq. (1) by estimating τ_l for $l = 1, \dots, L$. This can be done, e.g., by peak detection followed by Kalman filtering [9]. Hence, our algorithm treats each target independently, processing the CIR estimates for the corresponding path. For this reason, under the above assumption, the distinction among different paths does not pertain to the extraction of mD, so we simplify the notation by dropping the path index l , thus writing $\tilde{h}[w]$ to denote a CIR sample.

Our focus is reconstructing the mD spectrogram of the target from the Doppler domain channel \mathbf{H} , which corresponds to the Discrete Fourier Transform (DFT) of the CIR over the processing window. Particularly, if all the CIR samples in a window were available, \mathbf{H} could be obtained as $\mathbf{H} = \mathbf{F}^{-1} \mathbf{g}$ [3], where \mathbf{F} is the inverse Fourier matrix of dimension W , whose elements are $F_{nw} = e^{j2\pi n w / W} / \sqrt{W}$, $n, w \in \mathcal{W}$, while $\mathbf{g} = [\tilde{h}[0], \dots, \tilde{h}[W-1]]^T$ is the vector containing the CIR samples. However, ISAC systems do not typically transmit packets at a regular rate due to the communication protocol [2]. In the next section, we modify the problem formulation, generalizing it to the case of irregular CIR estimates, which can be modeled as missing samples from vector \mathbf{g} .

B. micro-Doppler sparse recovery problem

In ISAC systems, only a subset of CIR samples is available, since CIR estimation is performed (i) for communication packets, which enable channel equalization, and (ii) for sensing-only packets, which only contain channel estimation fields.

While the scheduling of sensing packets can be personalized, communication packets are sent at irregular times. Hence, reconstructing the mD spectrogram from communication packets only would result in severe artifacts that strongly degrade the system performance.

Given the sparsity of the CIR in the Doppler domain, mD reconstruction can be cast as a sparse recovery problem. To model irregular CIR estimation times, we assume that CIR estimates are only obtained at a subset of M instants out of W time-steps in the window, whose indices are collected in set $\mathcal{M} = \{i_m\}_{m=1}^M$. It holds that $\mathcal{M} = \mathcal{M}_c \cup \mathcal{M}_s$, where \mathcal{M}_c contains the CIR samples associated with communication packets, as specified in point (i) above, and \mathcal{M}_s includes the sensing samples (point (ii)).

We now denote by $\mathbf{M} = [\mathbf{e}_{i_m}^T]$, $\forall i_m \in \mathcal{M}$, the matrix that selects the rows of \mathbf{F} whose indices are in \mathcal{M} . Specifically, \mathbf{e}_i is the i -th element of the canonical basis, i.e., the vector of all zeros but the i -th component, which equals 1. Calling $\mathbf{h} = [\tilde{h}[i_1], \dots, \tilde{h}[i_M]]^T$ the vector containing the available CIR samples, we can write $\mathbf{h} = \mathbf{\Psi} \mathbf{H} + \mathbf{n}$, where $\mathbf{\Psi} = \mathbf{M} \mathbf{F}$ is the sensing matrix and \mathbf{n} is a noise vector.

A reconstruction of \mathbf{H} can be obtained by solving the following CS problem

$$\hat{\mathbf{H}} = \arg \min_{\mathbf{H}} \|\mathbf{h} - \mathbf{\Psi} \mathbf{H}\|_2^2 \quad \text{s.t.} \quad \|\mathbf{H}\|_0 \leq \Omega, \quad (3)$$

where Ω is the so-called *sparsity level* and determines the maximum number of non-zero components of \mathbf{H} . The above problem can be solved using iterative algorithms such as Iterative Hard Thresholding (IHT) or Orthogonal Matching Pursuit (OMP) [5]. Once $\hat{\mathbf{H}}$ has been obtained, the mD spectrum is computed as $\hat{\mathbf{D}} = |\hat{\mathbf{H}}|^2$.

C. Mutual coherence minimization

The most popular approach to designing sampling patterns that optimize CS reconstruction is to minimize the MC of the sensing matrix. The MC is defined as

$$\mu(\mathbf{\Psi}) = \max_{\substack{i,l=0,\dots,K-1 \\ i \neq l}} |\mathbf{\Psi}_i^H \mathbf{\Psi}_l|, \quad (4)$$

where $\mathbf{\Psi}_i$ and $\mathbf{\Psi}_l$ are the i -th and l -th columns of $\mathbf{\Psi}$, and \mathbf{X}^H represents the Hermitian of matrix \mathbf{X} . The MC measures the maximum correlation among the columns of $\mathbf{\Psi}$. Lower MC corresponds to better reconstruction performance using CS algorithms [6]. In general, MC decreases as more sensing samples are used for reconstructing the CIR spectrum, i.e. when M increases. However, the minimization of the MC is a combinatorial problem [6] for which an optimal solution can only be found for specific pairs of W and M [7]. In our scenario, W depends on the specific ISAC system, while M varies in time. Therefore, finding an optimal sampling pattern via mD minimization is infeasible, and approximate solutions are needed. Moreover, the ISAC setting introduces the following two technical challenges.

1) *Discrepancy between MC and sensing performance.* The quality of the CS reconstruction can be quantified by the Mean Squared Error (MSE) between the reconstructed mD and that

obtained from a complete CIR sampling window. However, an explicit relation between the MC and the MSE has not been proven and, as a result, a costly minimization of the MC could yield limited performance improvement. To achieve substantially better sensing performance, it would be desirable to select sampling patterns to *directly* enhance the MSE.

2) *Partial control over sampling patterns.* The CIR samples obtained from communication packets (\mathcal{M}_c) are not under control and their collection times are fixed. This means that \mathcal{M} can not be selected arbitrarily and only the locations of samples in \mathcal{M}_s can be scheduled to optimize MC. We stress that this is made even more challenging by the fact that the optimization of the sensing samples has to be *dynamically* carried out during system operation.

III. METHODOLOGY

In the following, we design a RL framework to select the sampling pattern in the target ISAC scenario. Our framework assumes that the communication packets' transmission instants become available at the start of each processing window. Hence, a RL agent has assigned the task of building the set \mathcal{M}_s with the final goal of minimizing the error between the true mD spectrum and the one reconstructed from the samples in \mathcal{M}_s by using the IHT algorithm [5].

A. Reinforcement learning model

We model the ISAC system as a Markov Decision Process (MDP) encoded by the tuple $(\mathcal{S}, \mathcal{A}, R, P, \gamma)$ [10]. In particular, \mathcal{S} is the state space, \mathcal{A} is the action space, $R : \mathcal{S} \times \mathcal{A} \times \mathcal{S} \rightarrow \mathbb{R}$ is the reward function, $P : \mathcal{S} \times \mathcal{A} \times \mathcal{S} \rightarrow [0, 1]$ is the transition probability function, and $\gamma \in [0, 1)$ is the *discount factor* that trades off between foresighted and myopic policies.

We consider that the processing of each window constitutes a distinct learning episode. At the start of the episode, the set \mathcal{M}_s is empty since no transmissions of sensing packets have been planned. Hence, each agent's action inserts a new sample within \mathcal{M}_s , and the agents continue to choose actions until the size of \mathcal{M}_s is equal to $M - |\mathcal{M}_c|$. We observe that the episode duration is variable and depends on the cardinality of \mathcal{M}_c , i.e., the number of communication packets that will be transmitted within the processing window.

We denote by $k = 0, 1, \dots, K - 1$ the time steps within the same episode, with $K = M - |\mathcal{M}_c|$. The state $s[k] \in \mathcal{S}$ observed at time k is modeled as a tuple $(\hat{\mathbf{H}}_{\text{prev}}, \mathcal{M}[k])$, where $\hat{\mathbf{H}}_{\text{prev}}$ is the Doppler-domain channel obtained at the end of the previous episode, while $\mathcal{M}[k]$ is the set \mathcal{M} after $k + 1$ agent decisions. This makes the state representation include two different components: $\hat{\mathbf{H}}_{\text{prev}}$, which does not vary in time, and $\mathcal{M}[k]$, which changes as the agent takes new decisions.

We remark that the choice to model the sample selection as a *sequential* decision-making problem is non-trivial and leads to significant advantages. A more intuitive, but naïve, approach is to use contextual Multi Armed Bandit (MAB) [10], where $\hat{\mathbf{H}}_{\text{prev}}$ represents the *context* observed by the agent and the action space is given by all the possible combinations of \mathcal{M} . However, this approach shares the same limitations of MC minimization, namely it requires performing optimization

over a combinatorial space. Indeed, the MAB action space contains all the possible combinations of sample instants selection over the available slots in the window, which has size $(W - |\mathcal{M}_c|)! / ((M - |\mathcal{M}_c|)! (W - M)!)$.

Unlike MAB, our framework upper bounds the cardinality of the action space by $W - |\mathcal{M}_c|$. Indeed, the agent's action space at slot k includes the indexes of all the idle samples so that $\mathcal{A}[k] = \mathcal{W} \setminus \mathcal{M}[k]$. If the agent chooses action a , the latter is added to the set \mathcal{M} and the environment evolves toward the state $s[k + 1] = (\hat{\mathbf{H}}_{\text{prev}}, \mathcal{M}[k + 1])$, where $\mathcal{M}[k + 1] = \mathcal{M}[k] \cup \{a\}$. This makes the MDP transitions deterministic, i.e., $s[k + 1]$ is fully predictable given $s[k]$ and $a[k]$.

Contrary to the transition probability function $P(\cdot)$, the reward function $R(\cdot)$ presents a stochastic behavior. Indeed, we make the reward depend on the true CIR spectrum, which is not part of the system state and whose reconstruction is the goal of the learning agent. Let us denote by $\hat{\mathbf{H}}[k]$ the estimation of the CIR spectrum that is obtained with IHT using $\mathcal{M}[k]$, i.e., all the samples selected up to time k . At step k , if the agent chooses action $a[k]$, the reward $r[k] = R(s[k], a[k], s[k + 1])$ is equal to

$$r[k] = \left(\text{MSE}(\hat{\mathbf{H}}[k + 1], \mathbf{H}) - \text{MSE}(\hat{\mathbf{H}}[k], \mathbf{H}) \right) / \|\mathbf{H}\|_2^2, \quad (5)$$

where $\text{MSE}(\mathbf{x}, \mathbf{y}) = \sum_{i=0}^{n-1} (x_i - y_i)^2 / n$ is the MSE between vectors \mathbf{x} and \mathbf{y} , while $\|\mathbf{x}\|_2$ is the Euclidean norm of \mathbf{x} .

In our system, the reward increases as the agent selects more useful samples for spectrum estimation. The agent decisions are determined by a policy $\pi : \mathcal{S} \times \mathcal{A} \rightarrow [0, 1]$, where $\pi(s, a)$ represents the probability of taking action a in state s . Hence, the agent's goal is to find the policy that maximizes the reward earned over each episode, given by the discounted return $G[k] = \sum_{\nu=k}^{K-1} \gamma^{\nu-k} r[\nu]$. Finally, we stress that the reward, and hence the ground-truth Doppler domain channel \mathbf{H} , is only used to *train* the agent while, during the inference, our system does not require the knowledge of \mathbf{H} .

B. Agent architecture and training

To make the agent find the optimal strategy, we use Proximal Policy Optimization (PPO), a *policy gradient algorithm* that allows us to concurrently estimate both the policy π , as defined in the previous section, and the state-value function $V_\pi : \mathcal{S} \rightarrow \mathbb{R}$. The latter associates each state s with the expectation $E_\pi[G[k] | s[k] = s]$ of the cumulative return obtained given that the agent follows policy π . More details about PPO can be found in the original paper [11].

To avoid the problems associated with the *curse of dimensionality*, we implement both the policy $\pi(\cdot)$ and the state-value function $V_\pi(\cdot)$ as Convolutional Neural Network (CNN) models. Both models take as input the state s that the agent observes while returning as output a single value, in the case $V_\pi(\cdot)$, and a probability distribution over the action space, in the case of $\pi(\cdot)$. The hidden architecture of the two models is the same and includes a sequence of 4 one-dimensional convolutions with a fixed kernel size (equal to 5), and an increasing channel number, which reaches the value of 32 in the last layer. Both models alternate the hidden layers

with rectified linear units as nonlinear activation functions and implement a feed-forward layer at the output. While the $V_\pi(\cdot)$ model ends with a simple linear combination, we add a *softmax* function at the end of the π model to ensure that the output corresponds to a probability distribution.

During the training phase, we make the agent interact with the environment for N_{train} windows. In doing so, we assume that $\hat{\mathbf{H}}_{\text{prev}}$, i.e., the spectrum reconstructed after processing the previous window, is identical to the ground truth so that $\hat{\mathbf{H}}_{\text{prev}} = \mathbf{H}$. This allows the agent to interact with an ideal environment at training time, with perfect information about the channel in the previous processing window. Conversely, during the test phase, which lasts N_{test} episodes, $\hat{\mathbf{H}}_{\text{prev}}$ is obtained using the samples chosen by the agent during the previous episode, as occurs in a real ISAC scenario.

IV. SETTINGS AND RESULTS

In this section, we validate our approach on real CIR traces and against existing methods from the literature. To this goal, we exploit the public DISC dataset [8], which contains 416 IEEE 802.11ay CIR sequences, obtained using a monostatic ISAC platform operating at 60 GHz carrier frequency. The CIR is estimated at a fixed sampling rate of $T_c = 0.27$ ms, using pilot signals based on Golay sequences with 1.76 GHz of bandwidth. No preprocessing is applied on the CIR estimates. For additional details on the experimental setting, we refer to [8]. The dataset contains signal reflections on 7 subjects performing four different activities: *walking*, *running*, *waving hands*, and *sitting down/standing up*. We remark that the PPO algorithm was trained directly on DISC, whose traces were preliminary split between training and testing sets.

A. Scenario settings

In our experiments, we set the window size to $W = 64$, and consider three possible cardinality for the set \mathcal{M} , i.e., $M \in \{8, 16, 32\}$. We obtain incomplete CIR measurement patterns by randomly removing samples from the DISC CIR sequences. To determine the samples associated with the transmissions of communication packets, we define a Markov chain with two states, named σ_i and σ_t , that establishes if a certain slot stays idle or belongs to \mathcal{M}_c . When a new window is processed, the first slot is assigned to any state according to the steady state probabilities, while the remaining slots are associated with σ_i or σ_t according to the chain evolution.

We write $p_{i,t}$ and $p_{t,i}$ to denote the probability of going from state σ_i to state σ_t , and vice versa. These probabilities depend on two additional parameters, b and d , and are defined as $p_{i,t} = dp_{t,i}/(W-d)$, $p_{t,i} = 1 - 1/b$, $p_{i,i} = 1 - p_{i,t}$ and $p_{t,t} = 1 - p_{t,i}$. Hence, b denotes the tendency of having a burst of consecutive communication slots, while d is the density of communication slots within the same window.

We generate multiple Markov chain configurations by selecting $b \in \{M/2, M, 2M\}$ and $d \in \{M/8, M/4, M/2\}$. For each configuration, we implement an ad hoc RL agent trained for $3 \cdot 10^4$ episodes and setting $\gamma = 0.99$. We exploit Adam as neural network optimizer [12], considering 10^{-3} and $5 \cdot 10^{-5}$ as the maximum *learning rate* for $\pi(\cdot)$ and $V_\pi(\cdot)$, respectively.

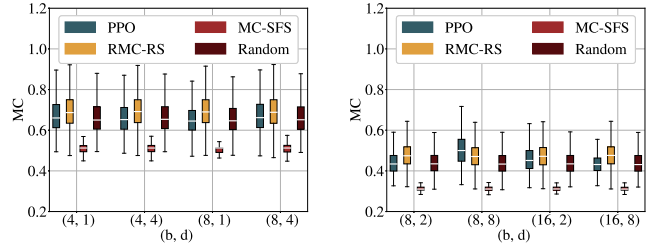


Fig. 1: Mutual Coherence (MC) for $M = 8$ (left) and $M = 16$ (right), considering $W = 64$ as windows length.

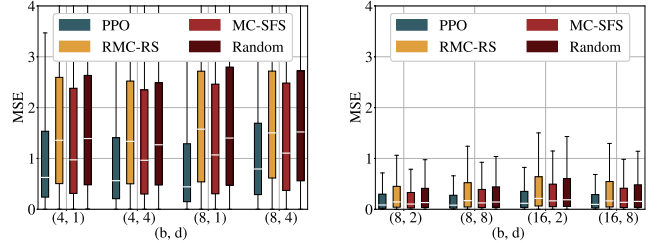


Fig. 2: Mean Squared Error (MSE) for $M = 8$ (left) and $M = 16$ (right), considering $W = 64$ as window length.

The PPO algorithm was tuned by using 0.1 as *clipping range* and 0.01 as *entropy coefficient*. During the test, we analyze 10 sequences of 250 windows each, which sets the total number of testing episodes to 2500.

We compare our RL framework against random sample selection and 2 recent algorithms from the literature, namely Mutual Coherence Sequential Forward Selection (MC-SFS) and Restricted Mutual Coherence Random Search (RMC-RS) [7]. The random policy selects the transmission instants of sensing packets according to a uniform distribution over the available slots in the processing window. Instead, MC-SFS follows a greedy approach to iteratively select the sample that minimizes the MC. Finally, RMC-RS exploits the last spectrum reconstruction, i.e., $\hat{\mathbf{H}}_{\text{prev}}$, to restrict the computation of the MC to a subset of columns of the sensing matrix; then, it randomly generates a set of different sampling patterns and selects the one that minimizes the MC. We specify that MC-SFS and RMC-RS were designed for settings where the sampling pattern can be freely chosen, i.e., $\mathcal{M}_c = \emptyset$. Therefore, we adapt MC-SFS and RMC-RS to our case by starting from the given set of samples \mathcal{M}_c and applying them to obtain the total sampling pattern selecting the remaining \mathcal{M}_s samples.

B. micro-Doppler reconstruction quality

To assess the performance of the different techniques, we consider both the MC and the MSE between the original and reconstructed spectrum. In Fig. 1, we represent the distribution of the MC using a boxplot representation, according to different scenario configurations. We observe that MC-SFS leads to the best performance in terms of MC in all the scenarios as it is explicitly designed to minimize it. PPO and random selection are agnostic to MC and thus present similar MC statistics. RMC-RS leads to even higher MC values, which may indicate

that such a technique is ineffective in our setting, due to the fast variation of the mD spectrum across time.

In terms of MSE, the proposed RL strategy leads to the best results and, in some circumstances, improves the median MSE obtained with MC-SFS by more than 40%. Looking at the percentiles of the MSE distribution, the benefits of the PPO algorithm are even more evident. For instance, considering $M = 8$, $b = 4$, and $d = 1$, the 75th percentile of the MSE distribution is about 1.5 with PPO, and 2.4 with MC-SFS. This confirms that optimizing MC does not guarantee higher mD quality, encouraging the use of learning strategies trained on minimizing MSE on real data. RMC-RS leads to very similar results to those obtained with the random selection and it is outperformed by both MC-SFS and PPO in all scenarios.

We observe that varying the Markov chain statistics (i.e., the values of b and d) does not substantially affect the results. Conversely, increasing M makes it possible to further reduce the MSE at the cost of transmitting more sensing packets. Finally, to visualize the benefits of the proposed approach, in Fig. 3, we represent an example of Doppler spectrogram reconstructed by PPO and MC-SFS, considering $M = 8$, $b = 8$, and $d = 1$. As highlighted in the dashed boxes, the mD obtained by PPO shows higher detail, which is useful for distinguishing different components in the spectrogram, and is less affected by background noise.

C. Computational complexity

In the following, we compare our approach to existing methods in terms of computational complexity. The random selection strategy does not optimize the sample selection, so its complexity is the lowest among the considered methods, requiring $\mathcal{O}(M)$ operations. As shown in [7], MC-SFS has a time complexity $\mathcal{O}(W^3M^3)$ due to the expensive computation of the MC via Eq. (4). Conversely, RMC-RS has complexity $\mathcal{O}(2^U U^2 M)$, where U is the number of non-zero components in the spectrum at the previous iteration. Finally, the proposed RL algorithm has a time complexity of $\mathcal{O}(YM)$, where Y denotes the number of operations performed by the CNN to select the samples in a processing window, which depends on the size of the learning architecture.

In Tab. 1, we report the median time, in milliseconds, spent by each technique to select a single sample to be inserted into \mathcal{M} . Random selection has the lowest complexity, spending about 0.03 ms per sample. The MC-SFS and RMC-RS have high computational costs due to the computation of the MC: in the scenario with $M = 8$, they require more than 15 ms and 46 ms per action, respectively. Appreciably, PPO strongly outperforms the benchmarks and requires less than 2 ms per sample in all configurations. This confirms how adopting data-driven approaches for CS-based mD reconstruction is beneficial in terms of both accuracy and computational efficiency.

V. CONCLUDING REMARKS

In this letter, we proposed a deep RL-based approach to select sensing packets transmission times in communication-centric ISAC for micro-Doppler (mD) reconstruction. Our framework sequentially selects the transmission times based

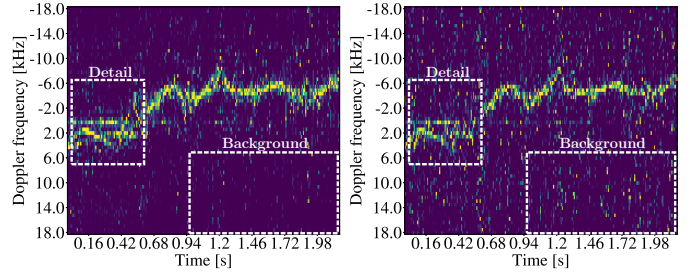


Fig. 3: Walking Doppler spectrum using PPO (left) and MC-SFS (right), with $(M, b, d) = (8, 8, 1)$. PPO shows higher detail and less background noise than MC-SFS, as shown in the dashed boxes.

(M, b, d)	PPO	RMC-RS [7]	MC-SFS [7]	Random
(8, 4, 1)	1.94	46.34	10.27	0.03
(8, 4, 4)	1.95	46.28	10.20	0.03
(8, 8, 1)	1.93	46.27	10.17	0.02
(8, 8, 4)	1.94	46.17	10.16	0.03
(16, 8, 2)	1.89	15.54	9.37	0.03
(16, 8, 8)	1.90	15.53	9.45	0.03
(16, 16, 2)	1.90	15.49	9.41	0.02
(16, 16, 8)	1.92	15.50	9.38	0.02

TABLE 1: Median time (in milliseconds) spent by each algorithm to identify a new candidate to be added to set \mathcal{M}_s .

on the available channel samples from communication packets and the last estimation of the mD spectrum. The framework is trained with the PPO algorithm to directly maximize the reconstruction quality, rather than the widely used MC metric from the literature. When tested on a real dataset of channel measurements, our system achieves up to 40% higher mD reconstruction accuracy and several times lower computational complexity compared to existing methods.

REFERENCES

- [1] F. Dong, F. Liu, Y. Cui, W. Wang, K. Han, and Z. Wang, "Sensing as a service in 6G perceptive networks: A unified framework for ISAC resource allocation," *IEEE Trans. Wirel. Commun.*, vol. 22, pp. 3522–3536, May 2023.
- [2] J. Pegoraro, J. O. Lacruz, M. Rossi, and J. Widmer, "SPARCS: A Sparse Recovery Approach for Integrated Communication and Human Sensing in mmWave Systems," in *21st ACM/IEEE International Conference on Information Processing in Sensor Networks (IPSN)*, (Milan, Italy), 2022.
- [3] B. Vandersmissen, N. Knudde, A. Jalalvand, I. Couckuyt, A. Bourdoux, W. De Neve, and T. Dhaene, "Indoor person identification using a low-power FMCW radar," *IEEE Trans. Geosci. Remote Sens.*, vol. 56, no. 7, pp. 3941–3952, 2018.
- [4] J. A. Zhang, M. L. Rahman, K. Wu, X. Huang, Y. J. Guo, S. Chen, and J. Yuan, "Enabling joint communication and radar sensing in mobile networks—A survey," *IEEE Commun. Surv. Tutor.*, vol. 24, pp. 306–345, January 2022.
- [5] Y. C. Eldar and G. Kutyniok, *Compressed sensing: theory and applications*. Cambridge University Press, 2012.
- [6] G. Xu and Z. Xu, "Compressed sensing matrices from Fourier matrices," *IEEE Trans. Inf. Theory*, vol. 61, pp. 469–478, January 2015.
- [7] Z. Song, Y. She, J. Yang, J. Peng, Y. Gao, and R. Tafazolli, "Nonuniform Sampling Pattern Design for Compressed Spectrum Sensing in Mobile Cognitive Radio Networks," *IEEE Trans. Mob. Comput.*, vol. 23, pp. 8680–8693, September 2024.
- [8] J. Pegoraro, J. O. Lacruz, M. Rossi, and J. Widmer, "DISC: a dataset for integrated sensing and communication in mmWave systems," *IEEE Dataport* <https://dx.doi.org/10.21227/2gm7-9z72>, 2022.
- [9] J. Pegoraro, J. O. Lacruz, F. Meneghello, E. Bashirov, M. Rossi, and J. Widmer, "RAPID: Retrofitting IEEE 802.11ay Access Points for Indoor Human Detection and Sensing," *Trans. on Mob. Comp.*, vol. 23, no. 5, pp. 4501–4519, 2024.

- [10] R. S. Sutton and A. G. Barto, *Reinforcement learning: An introduction*. MIT press, 2018.
- [11] J. Schulman, F. Wolski, P. Dhariwal, A. Radford, and O. Klimov, "Proximal Policy Optimization Algorithms," <https://arxiv.org/abs/1707.06347>, 2017.
- [12] D. P. Kingma and J. Ba, "Adam: A method for stochastic optimization," <https://arxiv.org/abs/1412.6980>, 2017.